Catalysis Today 171 (2011) 304–311

Contents lists available at ScienceDirect

Catalysis Today

journal homepage: www.elsevier.com/locate/cattod

Sour water–gas shift reaction over Pt/CeO_2 catalysts

Bing Liu, Andreas Goldbach*, Hengyong Xu*

Laboratory of Applied Catalysis, Dalian Institute of Chemical Physics, CAS, Dalian 116023, China

ARTICLE INFO

Article history:
Received 31 October 2010
Received in revised form 19 February 2011
Accepted 24 March 2011
Available online 4 May 2011

Keywords:
Water–gas shift
Sulfur tolerance
Platinum catalyst
Mesoporous ceria
Methanation

ABSTRACT

Ceria-supported catalysts with 0.38–2.0 wt.% Pt have been studied under high-temperature water–gas shift (WGS) conditions with and without 20 ppm H_2S present, which is a typical level in feed streams for WGS reactors in IGCC power plants. The effect of H_2S on CO conversion decreased with increasing temperature in the range 573–723 K and also with increasing Pt content. A 1 wt.% Pt catalyst exhibited excellent stability during a 300 h test at 673 K and GHSV = 7500 l kg^{-1} h^{-1} in an H_2S-charged feed with steam-to-CO ratio 2 as CO conversion remained stable around 73%. This was still close to the corresponding thermodynamic limit of 78.8%, which was reached under sulfur-free conditions. The Pt ionization degree in WGS-tested catalysts increased only slightly with the H_2S addition as the Pt^{2+} fraction grew from ca. 40% to 50% and the Ce oxidation states remained similar too. The bimodal pore structure of the mesoporous CeO_2 was also retained after WGS experiments although the effective surface area had declined by nearly 20% following the 300 h test in sour syngas. This and the concomitant decline of surface OH groups were likely caused by adsorption of H_2S and subsequent formation of surface sulfates and thus responsible for lowering the WGS activity of the ceria surface in the presence of H_2S. We propose that Pt centers can mitigate this effect through hydrogen spillover in their vicinity thus maintaining a high WGS activity of these catalysts in sour syngas.

1. Introduction

The conversion of CO to H_2 via the water–gas shift (WGS) reaction is an important step in many chemical processes including the production of H_2 from fossil fuels and biomass [1]. It is carried out as a two step process with two diverse temperature regimes in conventional industrial applications [2]. First, most of the CO is converted over a promoted ferrochrome (Fe/Cr) catalyst in high-temperature shift reactors operating typically between 583 and 723 K. Then a more active $Cu/ZnO/Al_2O_3$ catalyst is used in low-temperature shift reactors to further convert the remaining CO between 483 and 523 K. Another industrially employed catalyst contains cobalt and molybdenum sulfides as the active ingredients. Catalysts of this type are sulfur-tolerant and can be used in sulfur-containing "sour" gas streams [3].

The integrated gasification combined cycle (IGCC) is a process which cogenerates electricity, chemicals and fuel gases from coal, resulting in higher efficiency, reduced environmental pollution and lower costs [4]. The WGS reaction is a key step in the IGCC for adjusting the CO/H_2 ratio for CH_3OH and NH_3 synthesis. In a typical IGCC power plant the coal-derived syngas is desulfurized to approximately 20 ppm H_2S [5,6]. This level is too high for conventional low-temperature Cu WGS catalysts, which are usually operated in syngas containing less than 0.1 ppm sulfur [6]. High-temperature Fe/Cr catalysts are less sensitive to sulfur poisoning, but their already low activity decreases further upon sulfur exposure [7]. Cobalt and molybdenum sulfides on the other hand retain high WGS activity only if they remain totally sulfided, which requires sulfur levels on the order of 1000 ppm in the feed [8,9]. Hence, none of the WGS catalysts that are currently in industrial use is well suited for IGCC syngas and interest in sulfur-tolerant WGS catalysts is growing again.

The literature about the sour WGS reaction with less than 100 ppm H_2S present is scarce. In that range sulfur has only a minor effect on the activity of commercial Fe/Cr catalysts as indicated by a small negative H_2S reaction order between −0.2 and −0.3, and in general the activity is fully restored after removal of the contaminant [5,7,10]. For example, Xue et al. reported a 20% decrease in CO conversion at 623 K after addition of 50 ppm H_2S [10] and Hla et al. observed a similar impact of 33 ppm H_2S at 723 K [7]. Boon et al. carried out a detailed study on the influence of 11–35 ppm H_2S on the WGS kinetics of a Fe/Cr catalyst between 648 and 748 K and confirmed early studies by Bohlbro [11] showing that H_2S affects the reaction orders of all reactants already at these low contaminant levels [5]. Noble metal WGS catalysts are interesting alternatives in this context, because they are much more active than Fe/Cr catalysts and in general more tolerant to poisons such as sulfur [12], but studies are even rarer. Xue et al. [13] examined the WGS activity of

* Corresponding authors. Tel.: +86 8437 9229; fax: +86 411 8469 1570.
E-mail addresses: goldbach@dicp.ac.cn (A. Goldbach), xuhy@dicp.ac.cn (H. Xu).

0920-5861/$ – see front matter © 2011 Elsevier B.V. All rights reserved.
doi:10.1016/j.cattod.2011.03.050

a 1 wt.% Pt/ZrO_2 catalyst in the presence of 50 ppm H_2S at 573 K. The CO conversion declined after introduction of H_2S but remained stable during 4 h and was rapidly and fully restored to its original level once H_2S was removed from the feed. Luo and Gorte [14] studied the effect of SO_2 on the WGS activity of Pd/CeO_2 catalysts, which is significantly enhanced due to the redox activity of the rare earth oxide. They observed an activity decline after ex situ poisoning with SO_2 and attributed it to formation of cerium sulfates on the catalyst surface. These sulfates could be reduced by CO to Ce_2O_2S, but the latter – unlike Ce_2O_3 – could not be re-oxidized by H_2O or CO_2. Thus the activity loss was blamed on blocking of the support redox cycle. The decline in catalyst activity after ex situ poisoning might be misleading, however, because contaminant levels on the catalyst might remain much lower under actual reaction conditions.

Therefore we investigated the effect that H_2S has on the WGS reaction over Pt/CeO_2 catalysts at typical IGCC syngas contaminant levels. These catalysts exhibit much faster WGS kinetics at high temperatures than conventional Fe/Cr catalysts and unlike the latter they are not sensitive to air (non-pyrophoric). The activity tests were complemented with X-ray powder diffraction (XRD), temperature programmed reduction (TPR), infrared spectroscopy (IR) and X-ray photoelectron spectroscopy (XPS) and CO chemisorption as well as N_2 adsorption measurements.

2. Experimental

2.1. Catalyst preparation and characterization

10 g of CeO_2 were prepared by precipitation of 150 ml aqueous 0.39 M $Ce(NO_3)_6(NH_4)_2$ solution with about 60 ml aqueous 1 M $(NH_4)_2CO_3$ solution (both from Shanghai Chemical Reagent Company). The final solution's pH value was 8–9. The precipitate was aged for 2 h, washed, dried at 393 K and eventually calcined for 4 h at 773 K in air. One gram of the resulting CeO_2 was impregnated with 0.5 ml aqueous solution of H_2PtCl_6 (Beijing Chemical Plant, 0.0075 g/ml) and 0.6 ml H_2O to obtain a catalyst loading of 0.38% Pt. For preparation of catalysts with 1% and 2% Pt, 0.27 and 0.53 ml of a higher concentrated H_2PtCl_6 solution (0.0376 g/ml) were used combined with 0.83 and 0.57 ml H_2O, respectively. The samples were kept for 24 h at room temperature to evaporate the solvent. Then they were dried overnight at 393 K to remove remaining solvent followed by calcination in air at 773 K for 4 h. Thus Pt was quantitatively adsorbed by the support. Note that Pt contents are given in weight percentages throughout this work.

XRD patterns of the prepared samples were measured in the range 5–90° on a Philips CM-1 powder X-ray diffractometer (Cu K_α, $\lambda = 0.1543$ nm) operating at 40 kV and 40 mA. A NOVA 4000 automated physisorption instrument (Quantachrome) was used to measure N_2-adsorption isotherms of the samples at liquid N_2 temperature (77 K). About 200 mg sample were degassed in vacuum at 623 K for 3 h prior to the measurements to remove pre-adsorbed components. The specific surface area was determined from the linear portion of the Brunauer–Emmett–Teller (BET) plot. The pore-size distribution was calculated from the desorption branch of the adsorption isotherm using the Barrett–Joyner–Halenda (BJH) formula.

CO chemisorption experiments were carried out using an Autochem 2910 instrument (Micromeritics) equipped with a thermal conductivity detector (TCD). About 200 mg sample was reduced for 2 h in H_2 at 773 K, flushed with Ar for 2 h and then cooled to 323 K. Then 0.1 ml pulses of 5 vol.% CO/He were injected into the catalyst bed at 323 K until no CO was chemisorbed anymore and the chemisorbed amount was calculated from the number of consumed pulses.

TPR experiments were carried out using a quartz reactor. The sample (40 mg) was purged with 30 ml/min Ar while heating at a ramp rate of 10 K/min to 773 K and maintaining that temperature for 30 min to remove traces of water. After cooling to room temperature the sample was reduced in a flow of 5 vol.% H_2/Ar (30 ml/min) while heating from 293 to 1173 K at a rate of 10 K/min. The effluent gas was passed through a cooling trap to condense water produced during the reduction before it was fed through a gas chromatograph (SHIMADZU GC-8A) equipped with a TCD to measure H_2 consumption. CuO was reduced in the same way for quantitative calibration of the consumed H_2.

Fourier transform infrared (FTIR) spectroscopy was performed on a Bruker EQUINOX 55 instrument with a spectral resolution of 4 cm^{-1} to characterize sulfur species adsorbed on the catalysts. Wafer samples were formed by compressing approximately 50 mg of the undiluted catalyst powder at a pressure of 0.5 MPa and loaded into a gastight IR cell. The IR spectrum of the evacuated empty cell was used as background. The fresh 2% Pt/CeO_2 catalyst and the ones used in sulfur contaminated syngas were pretreated at 673 K for 30 min under vacuum to remove airborne surface contaminations and then cooled to room temperature for the measurement.

XPS spectra of the samples were recorded at room temperature with a VG Scientific ESCALAB Mark II instrument using Al K_α radiation ($h\nu = 1486.6$ eV, $U = 10.0$ kV). The power of the X-ray source was 100 W and the nominal resolution was better than 0.1 eV. The background pressure in the analyzing chamber was kept below 7.5×10^{-8} Torr. The Pt 4f, Ce 3d, S 2p, O 1s and C 1s spectra were acquired and the latter was set at 284.6 eV and taken as a reference for binding energy (BE) calibration. The software XPSPEAK was used to fit the XPS spectra using a mixture of Gaussian and Lorentzian functions in a 40/60 ratio and a Shirley background.

2.2. Catalytic activity measurements

Catalytic activity measurements were carried out at atmospheric pressure between 573–723 K and a gas hourly space velocity GHSV = 7500 l kg^{-1} h^{-1} using a fixed bed quartz reactor with an inner diameter of 8 mm. Temperature was measured with a thermocouple located in a capillary inside the catalyst bed. A dry syngas mixture (17.9% CO, 11.4% CO_2, 1.8% CH_4, 2.0% N_2, H_2 balance) and N_2 containing none or 250 ppm H_2S were combined in a gas mixing rig. This mixture was fed into a preheater where steam was injected with a calibrated syringe pump (Elite P230). The N_2 feed rate was always 8 ml/min while the combined feed rates of the syngas mixture and steam amounted to 92 ml/min. Thus the H_2S contamination level was fixed at 20 ppm in all sour WGS tests. The standard feed mixture contained 67.7 ml/min dry syngas and 24.3 ml/min steam corresponding to a steam-to-CO ratio S/CO = 2. In a typical experiment, 800 mg catalyst diluted with 400 mg quartz was heated to 723 K in N_2 before switching to the reaction mixture. The stability of the catalyst performance was evaluated at 673 K and S/CO = 2 for an extended period of time followed by measurements at other temperatures and S/CO ratios. Fresh catalyst samples were used for the measurements in both sulfur-free and contaminated syngas except for the catalyst with the lowest Pt loading. There H_2S was added at 673 K by switching from pure N_2 to the H_2S/N_2 mixture after the clean syngas tests and the stability and temperature-dependent activity tests were repeated. The hot, wet tail gas was passed through a gas chromatograph (SHIMADZU GC-14C) equipped with a flame photometric detector (FPD) for sulfur analysis before steam was condensed out in an ice-filled cooling trap. Then the dry tail gas was passed through a second gas chromatograph (SHIMADZU GC-8A) equipped with a TCD for CO, CO_2, and CH_4 analysis.

The conversion of CO (X_{CO}) and selectivity of CH_4 (S_{CH_4}) are given by:

$$X_{CO} = \frac{[CO_2]_{out}}{[CO]_{out} + [CO_2]_{out}} \quad (1)$$

and

$$S_{CH_4} = \frac{[CH_4]_{out} - [CH_4]_{in}}{[CO]_{out} + [CO_2]_{out} + [CH_4]_{out} - [CH_4]_{in}}. \quad (2)$$

$[CO]_{out}$, $[CO_2]_{out}$, $[CH_4]_{in}$ and $[CH_4]_{out}$ are the CO, CO_2, and CH_4 concentrations before and after reaction, respectively. The thermodynamic WGS equilibrium conversion $X_{eq,CO}$ was obtained from the WGS equilibrium concentrations $[CO]_{eq}$ and $[CO_2]_{eq}$ calculated with the program Gas_{eq} [15]:

$$X_{eq,CO} = \frac{[CO_2]_{eq}}{[CO]_{eq} + [CO_2]_{eq}} \quad (3)$$

3. Results

3.1. WGS activity tests

The temperature dependent WGS activity of the catalysts is shown in Fig. 1a at S/CO = 2 and with and without H_2S present. X_{CO} increased with Pt loading and approached the equilibrium curve for both samples with high Pt content above 623 K in the absence of H_2S. At this point CH_4 formation also became noticeable (Fig. 1b) and increased rapidly with temperature and Pt loading. CO conversion was considerably lower over the 0.38% Pt catalyst and approached equilibrium only at the highest temperature where CH_4 formation became again noticeable (Fig. 1b). The WGS activity dropped somewhat after addition of H_2S but remained close to the equilibrium curve for the highly loaded Pt catalysts above 673 K (Fig. 1a). Interestingly, CH_4 could not be detected anymore soon after H_2S addition indicating that the side reaction was completely suppressed. The effect of S/CO ratio on X_{CO} at 673 K is shown in Fig. 2a. The catalyst with the highest Pt loading reached the equilibrium conversion curve at all S/CO ratios. X_{CO} deviated increasingly from the curve with decreasing Pt loading and further after addition of H_2S. CH_4 formation in uncontaminated syngas declined noticeably with increasing S/CO ratio though it did not play a role at the lowest Pt loading (Fig. 2b).

Fig. 3 shows a 300 h stability test of the 1% Pt catalyst in the presence of H_2S at 673 K and S/CO = 2 corresponding with $X_{eq,CO}$ = 78.8%. CO conversion dropped quickly from 79.7% to 74.7% within 10 h, and then further to 73.3% after 100 h, but remained stable at that level for another 200 h. CH_4 formation fell below the detection level in less than 20 h. H_2S was the only sulfurous species detected by the FPD and it reappeared practically quantitatively at the reactor exit after a short induction period. For comparison, CO conversion was stable at 76.2% with 0.8% CH_4 selectivity during 100 h operation in sulfur-free syngas under otherwise the same experimental conditions.

3.2. Characterization of the catalysts

XRD patterns of the fresh and all WGS-tested catalysts contained only reflections due to the characteristic fluorite structure of CeO_2. This suggests that Pt was well dispersed on the catalyst and testing in sulfur-free and sour syngas did not change that. Results of the BET measurements and chemical adsorption on fresh and used 1% Pt catalyst samples are presented in Fig. 4 and Table 1. The catalyst exhibited type IV adsorption isotherms with hysteresis loops typical of mesoporous materials in all tests. Fig. 4b indicates a small fraction of well-defined, 3.7 nm wide pores that stands out from a broad pore distribution with maximum at 9.5 nm. The formation of

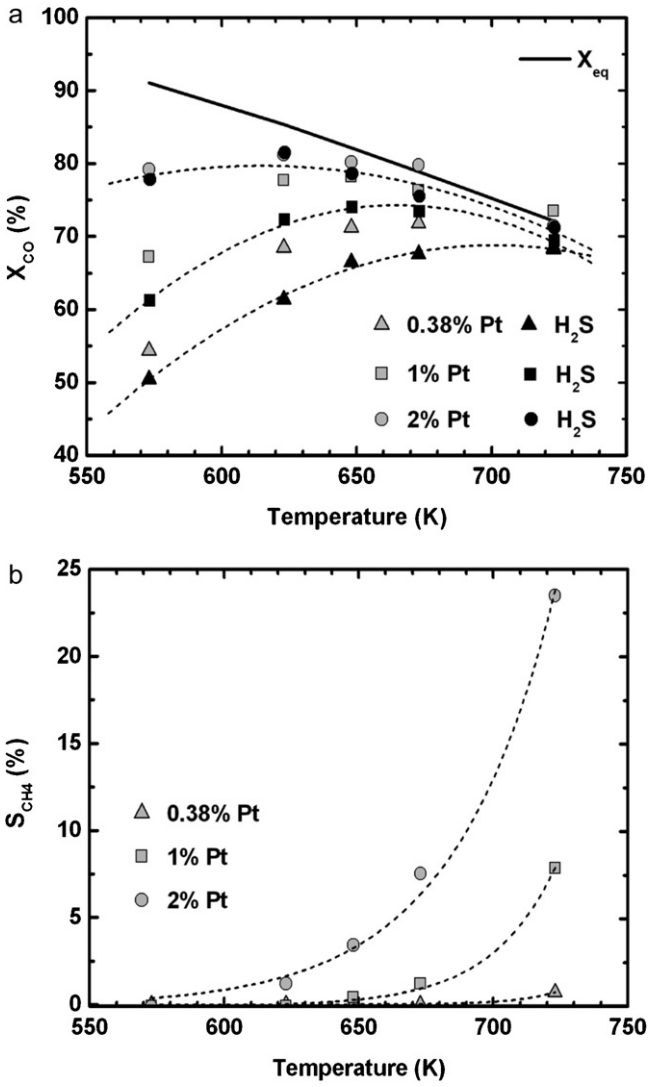

Fig. 1. Temperature dependence of (a) CO conversion and (b) CH_4 selectivity at S/CO = 2 over different Pt/CeO_2 catalysts with (solid symbols) and without H_2S (open symbols) present. The dashed lines are guides to the eye.

secondary smaller pores in mesoporous CeO_2 materials has been linked to the sintering and crystallization of ceria nanoparticles during calcination [16] and the presence of templates with different size during synthesis [17]. Interestingly, the bimodal pore distribution had not changed significantly after 100 h operation in sulfur-free or 300 h testing in H_2S-contaminated syngas. Pore volume, pore diameter and surface area of the catalyst tested in sulfur-free syngas were practically identical to those of the fresh sample, while the surface area was reduced by nearly 20% after the experiment in H_2S-charged syngas. This indicates that none of the

Table 1
Physicochemical characteristics of 1% Pt/CeO_2 catalysts tested under different conditions.

	Surface area (m^2/g)[a]	Pore volume (ml/g)[a]	Average pore diameter (nm)[a]	CO/Pt ratio[b]
Fresh	57.4	0.116	8.1	0.077
WGS (no H_2S)	55.9	0.110	7.9	0.104
WGS (H_2S)	48.2	0.108	9.0	0.083

[a] BET.
[b] CO adsorption.

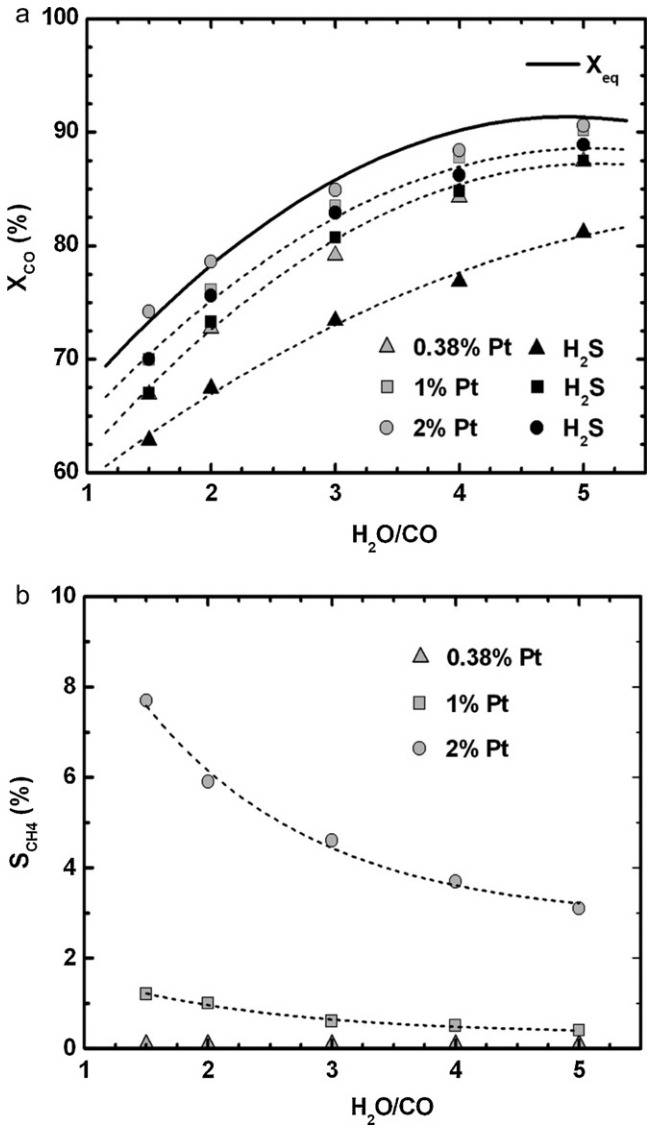

Fig. 2. Dependence of (a) CO conversion and (b) CH_4 selectivity on S/CO ratio over different Pt/CeO_2 catalysts at 673 K with (solid symbols) and without H_2S (open symbols) present. The dashed lines are guides to the eye.

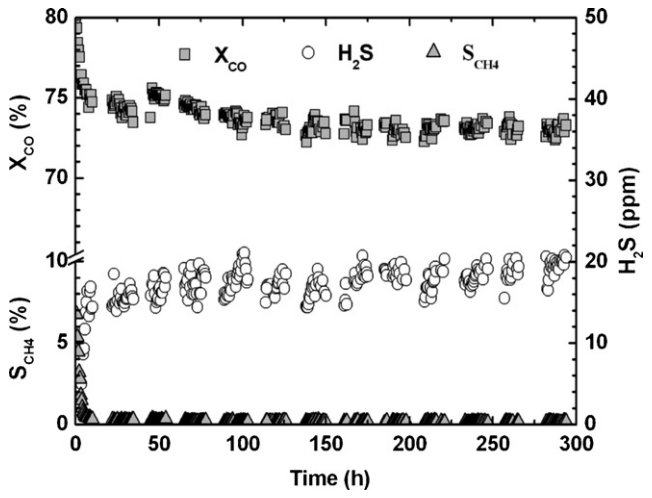

Fig. 3. 300 h stability test over 1% Pt/CeO_2 catalyst in the presence of 20 ppm H_2S at 673 K and S/CO = 2.

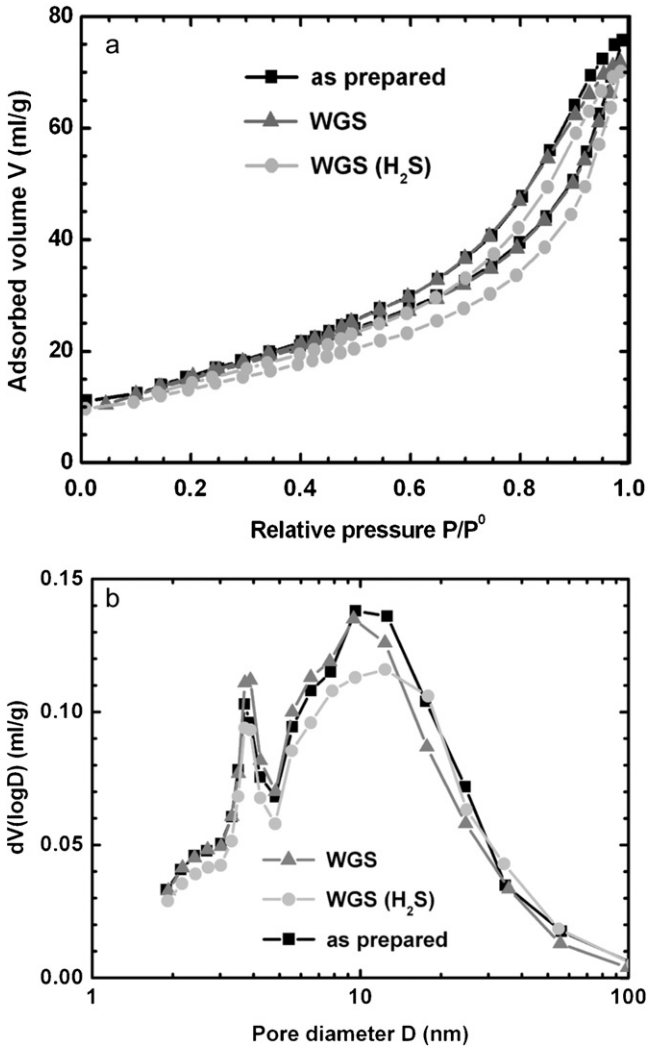

Fig. 4. (a) N_2 physisorption isotherms and (b) pore size distributions of fresh and used 1% Pt/CeO_2 catalyst samples (lines are guides to the eye).

reaction conditions affected the structure of the CeO_2 support itself although some surface sites appear to be blocked due to adsorption of sulfurous species.

Table 1 lists nominal CO/Pt ratios for the 1% Pt catalysts derived from CO chemisorption. These values are frequently used for determining the metal particle size on catalysts but the method can be misleading if the metal is supported on redox materials such as CeO_2 because of strong metal–support interaction (SMSI) [18] and reactive adsorption of CO at hydroxyl groups on the reduced ceria surface [19]. The latter effect leads to an underestimation of the metal particle size while the SMSI reduces the activity of Pt towards CO and results in too large particle size estimates. This was also the case in the present study. The CO/Pt ratios in Table 1 would suggest Pt particle sizes between 10 and 15 nm, which are clearly too large as the absence of Pt reflections in the XRD patterns implies Pt particles smaller than 5 nm. Hence the larger CO/Pt ratios after the WGS tests reflect the larger concentration of hydroxyl groups on the reduced ceria surface and possibly also changes in the SMSI rather than an unlikely decrease of the Pt particle size under WGS conditions. In this context it is interesting that the nominal CO/Pt ratio after the sour WGS test was 25% lower than that obtained after the sulfur-free WGS test. This is consistent with the decline of surface hydroxyl groups during the sour WGS reaction detected by XPS (vide infra).

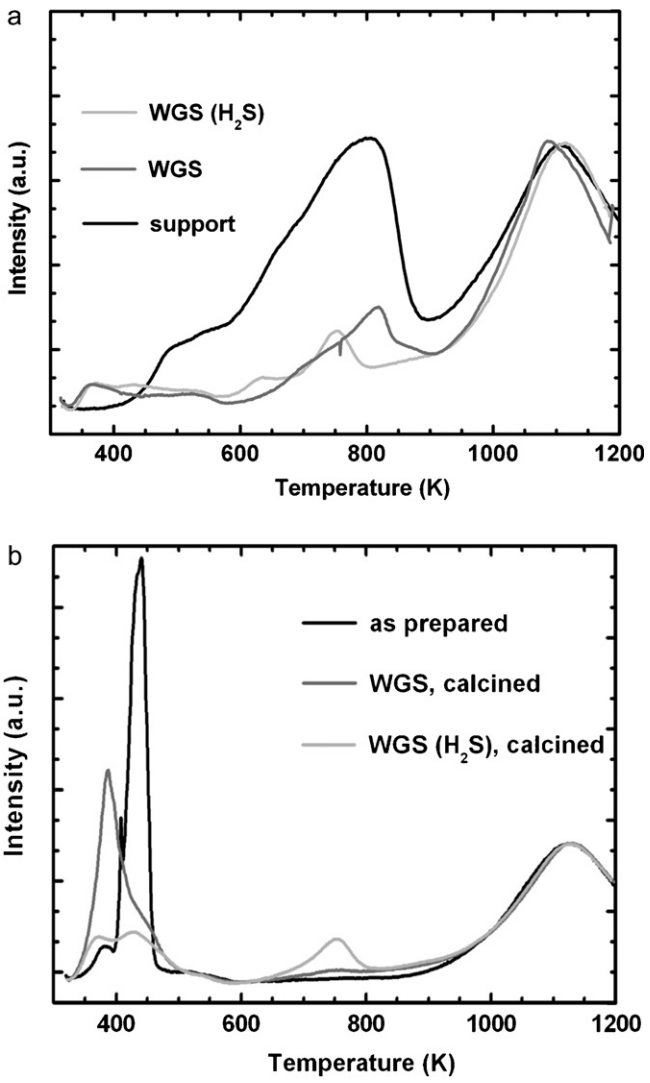

Fig. 5. (a) H_2-TPR profiles of 1% Pt/CeO_2 catalyst samples after WGS testing and calcined CeO_2 support and (b) of the fresh catalyst and the WGS-tested catalysts after calcination at 673 K in air for 2 h.

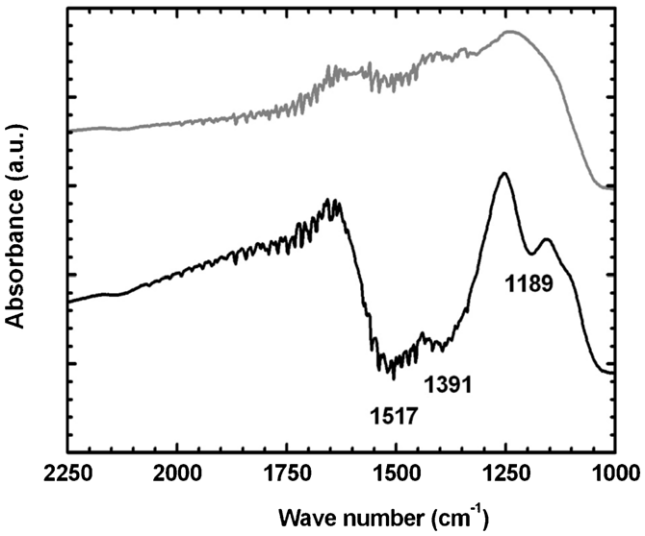

Fig. 6. FTIR spectra of the fresh 2% Pt/CeO_2 catalyst (grey trace) and after 100 h testing in syngas containing 20 ppm H_2S (black trace). The succession of small, narrow bands superimposed on the spectra between 1300 and 2000 cm^{-1} is likely due to gaseous H_2O trapped accidentally in the instrument.

Fig. 5a shows the H_2-TPR profiles of the 1% Pt catalysts used in WGS tests together with that of the CeO_2 support and Fig. 5b the corresponding profiles of the fresh and the calcined WGS-tested catalysts. The two broad H_2 consumption peaks of the support (Fig. 5a) stem from the reduction of bulk ceria (above 900 K) and surface ceria (400–850 K) [20]. Addition of Pt does not affect the reduction of bulk ceria but the surface ceria reduction peak is replaced by a narrow peak with a small low-temperature shoulder (fresh Pt catalyst in Fig. 5b). The shoulder can be attributed to the reduction of PtO to metallic Pt, which promotes CeO_2 surface reduction very efficiently yielding the intense reduction peak between 400 and 450 K [21]. These Pt-related features had disappeared after the WGS tests while H_2 consumption peaks reappeared between 600 and 900 K (Fig. 5a). However, the latter were much weaker than the corresponding one of the unpromoted support and they varied with H_2S, peaking around 820 K in the absence and at 750 K in the presence of H_2S.

Another portion of the catalysts used in the WGS tests was calcined for 2 h at 673 K in air before they were subjected to H_2 TPR. Fig. 5b shows that the H_2 consumption features between 600 and 900 K of the WGS-tested catalysts had disappeared following calcination except for a minor peak at 750 K from the catalyst used in sour syngas. This indicates that the latter peak does not result from surface ceria reduction. Very similar TPR reduction features were observed between 673 and 823 K after treatment of sulfated Pt/CeO_2 materials in a reducing atmosphere consisting of 2.5% H_2, 10% CO_2 and 10% H_2O in N_2 and attributed to the reduction of sulfate species [22]. This identification is supported by IR spectra. The spectrum of the 2% Pt catalyst, which had been tested for 100 h in sour syngas, is shown in Fig. 6 together with that of the fresh sample. The absorption bands at 1189 and 1391 cm^{-1} can be assigned to bulk sulfates and surface sulfates [23,24], respectively, with the latter clearly the dominant species, while that at 1517 cm^{-1} is likely due to surface carbonate [14]. The amount of deposited sulfur can be estimated from the difference between the TPR profiles of catalysts tested with and without H_2S present in the temperature range 573–823 K (Fig. 5b) [22], assuming a H_2/SO_4^{2-} ratio of 4 for the sulfate reduction (e.g. $SO_4^{2-} + 4H_2 \rightarrow S + 4H_2O + 2e^-$). The 0.5 μmol H_2 consumption difference corresponds to 0.01 wt.% S on the 1% Pt catalyst after the 300 h stability test and less than 0.2% of the total H_2S that was passed through the catalyst bed.

Fig. 5b also shows that the two Pt-related reduction peaks were restored after calcination of the WGS-tested catalysts albeit with varying intensities. The low-temperature shoulder of the fresh catalyst had turned into the dominant H_2 consumption feature after operation in sulfur-free syngas while the total H_2 consumption below 550 K remained very close to the value for the fresh catalyst (12 μmol). On the other hand both peaks had rather low intensities after the sour WGS test corresponding only to 5 μmol H_2 consumed altogether. This indicated that part of the ceria surface had been deactivated after H_2S exposure, which is consistent with the results of the BET and CO chemisorption measurements.

Fig. 7 shows the Pt 4f XPS spectra of the as prepared and 100 h WGS-tested 2% Pt catalysts and Figs. 8 and 9 the corresponding O 1s and Ce 3d spectra. Table 2 summarizes binding energies and relative concentrations of species derived from fitting of the Pt and O spectra. The Pt spectra could be well reproduced by two sets of spin-orbit doublets ($4f_{7/2}$ and $4f_{5/2}$ with an intensity ratio of 4:3) which can be assigned to Pt^0 and Pt^{2+}, respectively [25,26]. The Pt was in a mixed valence state after the WGS tests and the Pt^{2+} fraction was somewhat larger after the reaction with H_2S present. The O 1 s XPS spectra can be resolved into a main peak and a shoulder, which are attributed to lattice oxygen in ceria and surface hydroxyl species [27]. The OH concentration had grown after WGS testing although

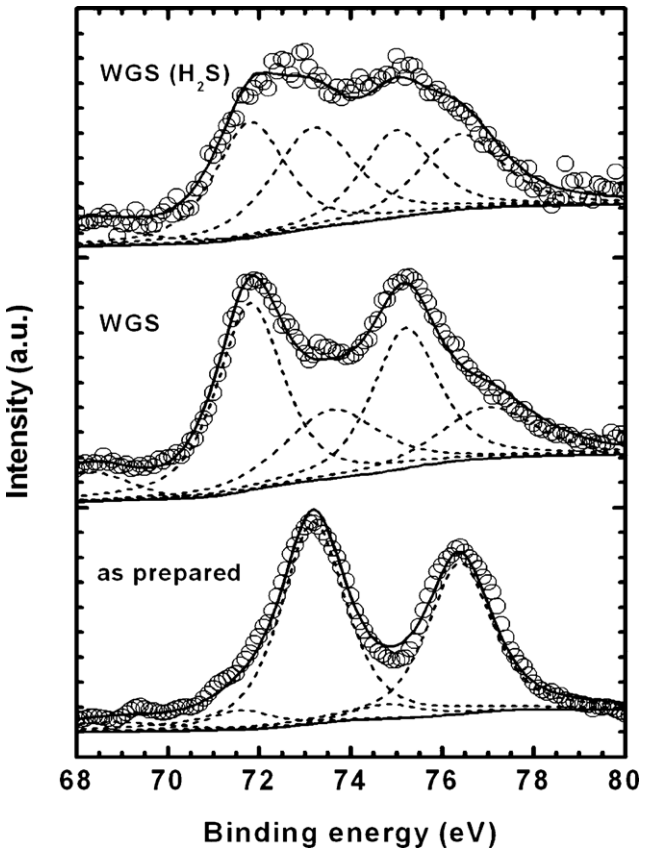

Fig. 7. Pt 4f XPS spectra of (a) the fresh 2% Pt/CeO_2 catalyst, (b) one tested in H_2S-free syngas, and (c) one tested in syngas with 20 ppm H_2S.

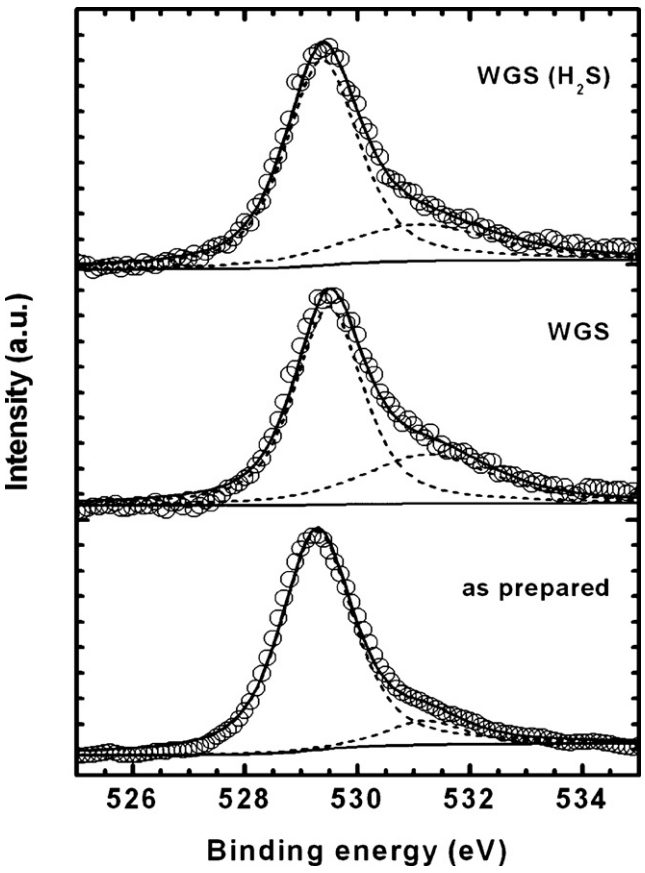

Fig. 8. O 1s XPS spectra of (a) the fresh 2% Pt/CeO_2 catalyst, (b) one tested in H_2S-free syngas, and (c) one tested in syngas with 20 ppm H_2S.

it did not increase as much in the presence of H_2S as in its absence. This suggests that the surface hydroxyl groups are involved in the reaction that produces the sulfate species detected by IR. Unfortunately, S 2p XPS signals could not be clearly detected due to the very small sulfur amounts trapped on the 2% Pt catalyst after the 100 h WGS test. Ce 3d XPS spectra of mixed valence ceria materials can be very complicated on the other hand due to the presence of 10 strongly overlapping transitions from six Ce^{4+} and four Ce^{3+} states [28]. The spectra obtained in the present study (Fig. 9) are not well resolved and very similar and thus do not lend themselves to straightforward interpretation. The leading peak at 882.0 eV is consistent with literature values for the dominant v transition of the Ce^{4+} states in Pt/CeO_2 catalysts [25,29]. The weak intensity gains around 885 and 904 eV in spectra of the WGS-tested catalysts are in the range where the Ce^{3+}-related v' and u' transitions occur [29] and thus might indicate a small and similar increase in that oxidation state after WGS reaction both in the presence and absence of H_2S.

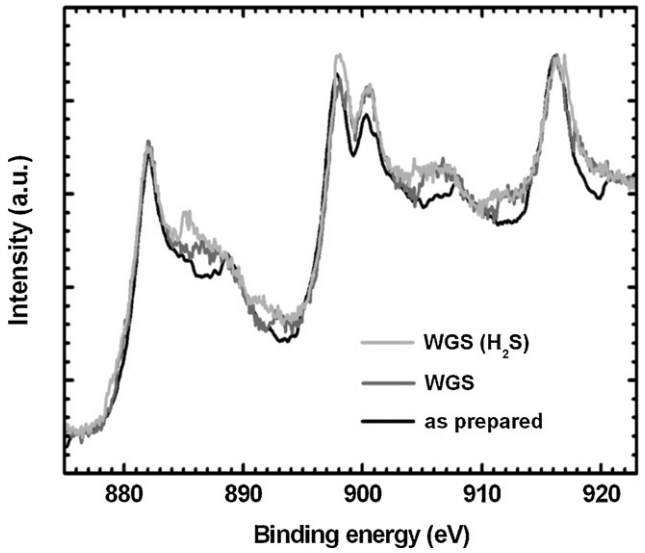

Fig. 9. Ce 3d XPS spectra of (a) the fresh 2% Pt/CeO_2 catalyst, (b) one tested in H_2S-free syngas, and (c) one tested in syngas with 20 ppm H_2S.

Table 2
Binding energies and atomic fractions x of Pt and O species in 2% Pt/CeO_2 catalyst tested under different conditions.

	Pt^0 $4f_{7/2}$		Pt^{2+} $4f_{7/2}$		Lattice O		OH	
	BE (eV)	x (%)	BE (eV)	x (%)	BE (eV)	x (%)	BE (eV)	x (%)
As prepared	71.6	11	73.2	89	529.2	89	531.2	11
WGS (no H_2S)	71.6	60	73.2	40	529.5	65	531.2	35
WGS (H_2S)	71.6	50	73.0	50	529.4	73	531.1	27

4. Discussion

The study by Xue et al. on a 1% Pt/ZrO_2 catalyst [13] is the only previous work on the performance of Pt catalysts under sour WGS conditions that we are aware of. They reported results from relatively short experiments (4 h) at just one temperature, i.e. 573 K, according to which CO conversion dropped from 58% to 44% at GHSV = 15,000 l kg^{-1} h^{-1} after addition of 50 ppm H_2S to a feed mix-

ture of 20% H_2O, 15% CO, 5% CO_2 and 5% H_2 in N_2. For comparison, X_{CO} declined from 67% to 61% over our 1% Pt/CeO_2 catalyst at that temperature after adding 20 ppm H_2S to a much less N_2-diluted feed (8% vs. 55%) with a large H_2 excess while S/CO was also 50% higher and the residence time twice as long in our experiments. The current study demonstrates that these noble metal catalysts retain a high activity also at higher temperatures under these conditions. The 300 h test further shows that this activity can be well maintained at typical IGCC syngas H_2S contamination levels as CO conversion became stable after ca. 100 h. This suggests that an equilibrated state was reached and catalyst deactivation came to a standstill after an induction period.

It is well established that CO conversion over the here studied catalysts involves both the Pt centers and the ceria surface with CO oxidation proceeding on the ceria surface [19,30–32]. The role of Pt is to promote the surface reduction of ceria to generate active OH groups [30,31]. It has been also proposed that it assists the dehydrogenation of reaction intermediates like formate and carbonate [19,32]. Details of the reaction mechanism and the relative importance of intermediate species are still under debate with the rate limiting step likely depending on reaction conditions [32]. It has been proposed that carbonate decomposition is the critical step at low temperatures and high CO_2 concentrations while formate decomposition dominates the kinetics at intermediate temperatures and high water concentrations [32]. At high temperatures in the presence of high H_2O concentrations and under conditions where the catalyst surface is mainly in an oxidized state, the decomposition of these intermediates should be very fast so that redox processes involving the ceria surface could be rate determining [32].

The relatively low stability of PtS likely plays a significant role in the good H_2S tolerance of these noble metal catalysts. Xue et al. reported that the formation of PtS was inhibited on the zirconia supported catalyst under WGS conditions [13] and neither did we obtain evidence for the formation of this or another sulfurous Pt compound. Thus, sulfidation of the catalytic noble metal centers can be dismissed as cause for the WGS activity loss after H_2S introduction. It is not clear whether the slightly larger Pt^{2+} fraction is related to the deactivation during sour WGS testing but we note that the WGS activity of certain Pt/CeO_2 catalysts has been found to increase with ionization degree [33].

However, the surface characteristics of the ceria support are crucial for the WGS activity of Pt/CeO_2 catalysts too. Luo and Gorte [14] attributed the WGS activity decline of Pd/CeO_2 catalysts after ex situ poisoning with SO_2 to blocking of the support surface redox cycle due to irreversible formation of Ce_2O_2S. We found no evidence for cerium oxysulfilde rendering this particular deactivation scenario improbable for Pt/CeO_2 under the conditions of the present study. Instead, the lower catalyst activity in the presence of H_2S could be related to the decrease of the CeO_2 surface during sour WGS testing. From the N_2 adsorption measurements it is clear that the pore architecture of the mesoporous ceria was very well preserved after both sulfur-free and sour WGS testing. Simultaneous blocking of small and large support pores due to collapse or sulfurous deposits can be practically excluded as the cause for the diminished surface area following sour WGS therefore. It is more likely that some (catalytic) adsorption sites disappeared on the CeO_2 surface in the latter case because of irreversible sulfur adsorption and/or reactions with the contaminant.

The decline of both the amount of surface oxygen (Fig. 5b) and the related fraction of surface hydroxyl groups (Table 2) under sour WGS conditions provide a clue about the catalyst deactivation mechanism in the presence of H_2S. It has been proposed that bridging hydroxyl groups on the partially reduced ceria surface are the catalytically active sites in Pt/CeO_2 WGS catalysts [30,31]. These OH groups are typically defect-associated and form via dissociative water adsorption. Their concentration depends on the equilibrium between water and competing species at vacant oxygen ion sites on the ceria surface [32]. H_2S has certainly a strong affinity towards these oxygen vacancies and likely interferes significantly with hydroxyl formation there. The resulting thiol groups are apparently susceptible to oxidation resulting in the formation of surface sulfates (Fig. 6). Note that ceria surface sulfate species are rather stable in reducing atmospheres at the temperatures covered in this study [22,24]. Experiments with pre-sulfated CeO_2 materials showed that complete reduction of these species depends strongly on the surface characteristics and can take several days at 673 K in H_2 atmosphere [24].

Pt promotes the generation of active hydroxyl groups [30,31] and it could also mitigate the inhibition of OH formation on the ceria surface if H_2S is present. Pt lowers the sulfate reduction temperature and accelerates the process significantly, though complete removal of SO_4^{2-} still remains a matter of hours at the temperatures investigated here [24]. Nevertheless, Pt destabilizes sulfates and it is plausible that it impedes their formation and H_2S adsorption in its neigborhood under WGS conditions. Pt maintains higher surface hydrogen concentrations in its vicinity through hydrogen spillover, which could slow down the dehydrogenation of H_2S on the CeO_2 surface facilitating H_2S redesorption before a thiol group can form. Thus oxygen vacancies would remain accessible for H_2O and a dynamic equilibrium would result between OH and SH groups nearby Pt centers. In this way the catalytic activity of the ceria surface could be preserved to a significant degree around the Pt centers as observed in the sour WGS experiments. Note that this mechanism can also account straightforward for the improvement of sulfur tolerance with catalyst Pt loading if the Pt center density increases in parallel, which is a reasonable assumption [34].

5. Conclusion

Ceria-supported Pt catalysts exhibit excellent activity for WGS conversion of sour syngas containing sulfur levels typical for IGCC power plants. CO conversion over a catalyst with 1% Pt stabilized at ca. 73% ($X_{eq,CO}$ = 78.8%) within the first 100 h of a 300 h test at 673 K and S/CO = 2 in syngas charged with 20 ppm H_2S. This suggests that S-induced catalyst deactivation comes to a halt within that time span. After 300 h less than 0.2 wt.% of the total sulfur passed through the catalyst bed had been trapped on the Pt/CeO_2, equaling 0.01 wt.% of the catalyst. The Pt and Ce oxidation states of catalysts tested in sulfur-free and sour syngas were similar, and neither was the bimodal mesopore structure of the support affected by those tests, showing that the catalyst architecture remained intact under all experimental conditions. The initial deterioration of the CO conversion during the 300 h test can be linked to the parallel decline of the surface area, the total amount of surface oxygen and the fraction of surface OH groups caused by competitive adsorption of H_2S and subsequent formation of sulfates on the CeO_2 surface during sour WGS. These processes are probably hindered in the neighborhood of Pt species due to hydrogen spillover keeping the catalyst highly active for WGS reactions even in the presence of H_2S. This renders Pt/CeO_2 catalysts promising alternatives to Fe/Cr catalysts for sour WGS, in particular if very high catalyst activities are required as in WGS membrane reactors. Those are currently intensely studied as a means to pre-combustion CO_2 capture in natural gas-fired power stations [35]. The efficiency of such membrane reactors can be vastly improved by incorporation of catalysts with faster WGS kinetics [36] and the availability of sulfur-tolerant catalysts will be critical for the implementation of these novel reactors in coal-based power generation schemes.

Acknowledgement

The authors gratefully acknowledge fruitful discussions with Profs. W.Z. Li and Q.J. Ge and financial support from the Ministry of Science and Technology of China (Grant No. 2005CB221401).

References

[1] Q. Fu, H. Saltsburg, M. Flytzani-Stephanopoulos, Science 301 (2003) 935.
[2] Y.T. Kim, E.D. Park, H.C. Lee, D. Lee, K.H. Lee, Appl. Catal. B 90 (2009) 45.
[3] M. Laniecki, M. Ignacik, Catal. Today 116 (2006) 400.
[4] S. Rezvani, Y. Huang, D. McIlveen-Wright, N. Hewitt, J.D. Mondol, Fuel 88 (2009) 2463.
[5] J. Boon, E. van Dijk, Ö. Pirgon-Galin, W. Haije, R. van den Brink, Catal. Lett. 131 (2009) 406.
[6] M.C. Carbo, J. Boon, D. Jansen, H.A.J. van Dijk, J.W. Dijkstra, R.W. van den Brink, A.H.M. Verkooijen, Int. J. Greenhouse Gas Control 3 (2009) 712.
[7] S.S. Hla, G.J. Duffy, L.D. Morpeth, A. Cousins, D.G. Roberts, J.H. Edwards, Catal. Commun. 10 (2009) 967.
[8] M. Łaniecki, M. Małecka-Grycz, F. Domka, Appl. Catal. A 196 (2000) 293.
[9] A.A. Andreev, V.J. Kafedjiysky, R.M. Edreva-Kardjieva, Appl. Catal. A 179 (1999) 223.
[10] E. Xue, M.O. Keeffe, J.R.H. Ross, Catal. Today 30 (1996) 107.
[11] H. Bohlbro, Acta Chem. Scand. 17 (1963) 1001.
[12] R. Farrauto, S. Hwang, L. Shore, W. Ruettinger, J. Lampert, T. Giroux, Y. Liu, O. Ilinich, Annu. Rev. Mater. Res. 33 (2003) 1.
[13] E. Xue, M. O'Keeffe, J.R.H. Ross, Stud. Surf. Sci. Catal. 130 (2000) 3813.
[14] T. Luo, R.J. Gorte, Catal. Lett. 85 (2003) 139.
[15] http://www.arcl02.dsl.pipex.com/.
[16] K. Suzuki, A.K. Sinha, J. Mater. Chem. 17 (2007) 2547.
[17] T. Brezesinski, C. Erpen, K. Iimura, B. Smarsly, Chem. Mater. 17 (2005) 1683.
[18] S. Bernal, J.J. Calvino, M.A. Cauqui, J.M. Gatica, C. López Cartes, J.A. Pérez Omil, J.M. Pintado, Catal. Today 77 (2003) 385.
[19] G. Jacobs, S. Ricote, U.M. Graham, P.M. Patterson, B.H. Davis, Catal. Today 106 (2005) 259.
[20] H.Q. Zhu, Z.F. Qin, W.J. Shan, W.J. Shen, J.G. Wang, J. Catal. 225 (2004) 267.
[21] S.M. de Lima, R.C. Colman, G. Jacobs, B.H. Davis, K.R. Souza, A.F.F. de Lima, L.G. Appel, L.V. Mattos, F.B. Noronha, Catal. Today 146 (2009) 110.
[22] N. Le Phuc, E.C. Corbos, X. Courtois, F. Can, P. Marecot, D. Duprez, Appl. Catal. B 93 (2009) 12.
[23] M. Waqif, P. Bazin, O. Saur, J.C. Lavalley, G. Blanchard, O. Touret, Appl. Catal. B 11 (1997) 193.
[24] P. Bazin, O. Saur, J.C. Lavalley, G. Blanchard, V. Visciglio, O. Touret, Appl. Catal. B 13 (1997) 265.
[25] S. Damyanova, B. Pawelec, K. Arishtirova, M.V.M. Huerta, J.L.G. Fierro, Appl. Catal. B 89 (2009) 149.
[26] X.L. Tang, B.C. Zhang, Y. Li, Y.D. Xu, Q. Xin, W.J. Shen, J. Mol. Catal. A 235 (2005) 122.
[27] O. Pozdnyakova, D. Teschner, A. Wootsch, J. Krohnert, B. Steinhauer, H. Sauer, L. Toth, F. Jentoft, A. Knop-Gericke, Z. Paal, R. Schlögl, J. Catal. 237 (2006) 1.
[28] A.I. Boronin, E.M. Slavinskaya, I.G. Danilova, R.V. Gulyaev, Y.I. Amosov, P.A. Kuznetsov, I.A. Polukhina, S.V. Koscheev, V.I. Zaikovskii, A.S. Noskov, Catal. Today 144 (2009) 201.
[29] E.L. Wilson, Q. Chen, W.A. Brown, G. Thornton, J. Phys. Chem. C 111 (2007) 14215.
[30] T. Shido, Y. Iwasawa, J. Catal. 141 (1993) 71.
[31] G. Jacobs, U.M. Graham, E. Chenu, P.M. Patterson, A. Dozier, B.H. Davis, J. Catal. 229 (2005) 499.
[32] R. Burch, Phys. Chem. Chem. Phys. 8 (2006) 5483.
[33] P.A. Deshpande, M.S. Hedge, G. Madras, Appl. Catal. B 96 (2010) 83.
[34] Y.H. Zhou, J.M. Perket, J. Zhou, J. Phys. Chem. C 114 (2010) 11853.
[35] D. Jansen, J.W. Dijkstra, R.W. van den Brink, T.A. Peters, M. Stange, R. Bredesen, A. Goldbach, H.Y. Xu, A. Gottschalk, A. Doukelis, Energy Proc. 1 (2009) 253.
[36] Y.D. Bi, H.Y. Xu, W.Z. Li, A. Goldbach, Int. J. Hydrogen Energy 34 (2009) 2965.